Rate of Reduction of Ore-Carbon Composites: Part II. Modeling of Reduction in Extended Composites

O.M. FORTINI and R.J. FRUEHAN

A new process for ironmaking was proposed using a rotary hearth furnace and an iron bath smelter to produce iron employing wood charcoal as an energy source and reductant. This paper examines reactions in composite pellet samples with sizes close to sizes used in industrial practice (10 to 16 mm in diameter). A model was constructed using the combined kinetic mechanism developed in Part I of this series of articles[1] along with equations for the computation of pellet temperature and shrinkage during the reaction. The analysis of reaction rates measured for pellets with wood charcoal showed that heat transfer plays a significant role in their overall rate of reaction at elevated temperatures. The slower rates measured in pellets containing coal char show that the intrinsic kinetics of carbon oxidation is more significant than heat transfer. Model calculations suggest that the rates are highly sensitive to the thermal conductivity of pellets containing wood charcoal and are less sensitive to the external conditions of heat transfer. It was seen that the changes in pellet surface area and diameter due to shrinkage introduce little change on reaction rates. The model developed provides an adequate description of pellets of wood charcoal up to circa 90 pct of reduction. Experimentally determined rates of reduction of iron oxide by wood charcoal were approximately 5 to 10 times faster than rates measured in pellets with coal char.

I. INTRODUCTION

IN Part I of this series of articles,[1] a new process for ironmaking was proposed using a rotary hearth furnace (RHF) in combination with a smelter. In the new process, composite pellets of iron oxide and carbon would be partially reduced in a rotary hearth furnace, and the final reduction, melting, and gangue separation would be done in the smelting unit. The rate constants for oxidation of wood charcoal and graphite by CO_2 and reduction of wustite by CO were measured at temperatures relevant to the RHF. In this article, a model for the reduction of composite pellets is developed taking into account the combined kinetics of carbon oxidation and wustite reduction along with heat transfer and pellet shrinkage. The modeling for this system was done coupling the equations of continuity for solid and gas with an enthalpy balance applied to a control volume inside the pellet. Experimentally, measurements of mass change, pellet size, and composition of off-gas during reduction were done in order to validate the model. The final model was used in a process model of the RHF.[22]

A number of models can be found in the literature, which are related to reduction in composites of iron oxides and carbon.[2,3,6–9] The main features commonly found in the reduction models are reaction rate laws, temperature change, gas transport, and changes in size of specimen. A summary of the approaches found in the literature for each of these items is given in Table I. The interested reader is referred to the original authors for the specifics of their individual contributions. In here, only an outline of the major differences in approach between authors is given.

O.M. FORTINI, Senior Research Engineer, is with the U.S. Steel Research and Technology Center, Monroeville, PA 15146. R.J. FRUEHAN, Professor, is with the Materials Science and Engineering Department, Carnegie Mellon University, Pittsburgh, PA 15213. Contact e-mail: fruehan@andrew.cmu.edu

Manuscript submitted April 7, 2004.

Reaction rate laws: The generally accepted mechanism of reduction in composites of iron oxides and carbon consists of two elementary reaction steps: carbon oxidation and reduction of iron oxides. The two steps were discussed in Part I of this series of articles. Consistent with this reaction mechanism, Rao[2] and Tien and Turkdogan[3] presented models for reduction in composites where the overall kinetics is controlled by the oxidation of carbon. This should be the case at lower temperatures, where rates of reduction of iron oxides are considerably faster than rates of carbon oxidation. Rao used a rate law in the original form derived from the mechanisms of Gadsby *et al.*[4] and Reif,[5] while Tien and Turkdogan employed a simplified version to account for the effects of poisoning by CO. Sohn and Szekely[6] suggested the use of a form similar to that used by Tien Turkdogan with the addition of a reversible term for both steps of carbon oxidation and reduction of the iron oxides. In the modeling of reactions at higher temperatures, Sun and Lu[7,8] and Donskoi and McKelwain[9] considered both steps in the reaction mechanism in the formulation of reaction rate laws. Sun and Lu applied a rate law for reduction of iron oxides expressing the surface of carbon available for reaction in terms of a geometric factor relating area to average size of carbon particles in the aggregate. It is interesting to notice that Sun and Lu also used the same form of rate law for the oxidation of carbon. In a different approach, Donskoi and McKelwain used a series of "mass ratio coefficients" assuming a first-order reaction with no direct address to mechanisms of carbon oxidation. The values or procedures for determination of the mass ratio coefficients were not specified in the work of Donskoi and McKelwain.

Reaction sequence: Rao[2] and Sun and Lu[7,8] assume a stepwise pattern of reduction where each step in the sequence $Fe_2O_3 \rightarrow Fe_3O_4 \rightarrow FeO \rightarrow Fe$ goes to completion before the next step is started. Tien Turkdogan[3] and Donskoi and McKelwain[9] do not rely on this hypothesis. Some authors have observed the coexistence of more than two iron phases during reduction of composites, but it is unclear whether the three phases were found in the same grain or in different

Table I. Main Characteristics of Previous Models of Reduction in Composites of Iron Oxides and Carbon

Author	Kinetic Mechanism	Temperature Change	Gas Transport	Size Changes
Sun and Lu[7]	mixed control	nonisothermal	molecular diffusion and forced flow	not addressed
Rao[2]	carbon oxidation control	isothermal	Knudsen diffusion	not addressed
Tien and Turkdogan[3]	carbon oxidation control	isothermal	molecular diffusion	not addressed
Sohn and Szekely[6]	mixed control	isothermal	not addressed	not addressed
Sun and Lu[8]	mixed control	nonisothermal	Ergun (laminar)	not addressed
Wang *et al.*[11]	direct reduction	nonisothermal	not addressed	not addressed
Donskoi and McElwain[9]	empirical arrenius laws	nonisothermal	not addressed	addressed with empirical correlations

locations inside the reacting mixture. The coexistence of more than two iron phases was experimentally verified by Spitzer *et al.*[10] for the reduction of large specimens of iron oxides in streams of reducing gases (CO, H_2).

Temperature change: The temperature change is usually determined by means of an enthalpy balance. Simple formulations can be found in the literature[11] where no temperature gradient inside the samples is considered. In other works, such as those of Sun and Lu[7,8] and Donskoi and McKelwain,[9] the enthalpy balance is usually done considering the distribution of temperatures inside the reacting mixture or pellet. In the early work of Sun and Lu[7] and in the work of Dosnkoi and McKelwain, no account is taken of the gas transport in the enthalpy balance. However, in the most recent work, Sun and Lu[8] include such transport of gas.

Gas transport: The problem of gas transport inside reacting composites has been approached in at least two different ways. Rao[2] assumed that Knudsen diffusion was the operative mode of gas transport and derived expressions for the effective Knudsen diffusivity based on structural parameters of the reacting composite. Tien and Turkdogan[3] and Lu[8] considered the movement of gas as the result of molecular diffusion and forced flow due to the positive net rate of gas generation during reduction. Other researchers such as Donskoi and McKelwain[9] consider the transport of gas as secondary for the overall reduction process, thus disregarding gaseous exchanges in their formulation.

Changes in pellet size: Changes in size of reacting composites have been addressed essentially by means of empirical correlations, as exemplified in the work of Donskoi and McKelwain.[9] In their work, Donskoi and McKelwain considered the total change in size of the reacting composite as the combined result of shrinkage and swelling with proper empirical correlations derived from works of other researchers. It must be noticed that the empirical correlations used are obtained assuming an isothermal situation where the composite sample is at a given temperature during the entire process. The use of such correlations in cases where the samples are nonisothermal may not be strictly correct. No attempt for a more refined treatment of changes in size could be found in the literature.

II. EXPERIMENTAL APPARATUS AND TECHNIQUE

The apparatus used in this research, a thermogravimetric furnace, was described in Part I of this series of articles. In the current work, reduction experiments were done with composite pellets of carbon and iron oxides following the same procedure described previously.[1] The samples were in the form of pellets of 10 to 16 mm. Three different types of carbon and two types of iron oxides were employed: wood charcoal, coal, graphite, ore, and reagent grade hematite. The amount of ash in the wood charcoal used was measured by burning samples of sized granules (from larger than 20 mesh down to smaller than 200 mesh) in a muffle furnace under air. In these tests, the samples were placed in crucibles and had their mass measured in intervals of 24 hours until no measurable mass loss could be registered for three consecutive intervals. These experiments showed a low amount of ash (less than 2 pct) in the wood charcoal. A maximum of 1.7 pct in mass of ash was found in the wood charcoal fraction smaller than 200 mesh. The amount of ash in the coal was significantly higher than in wood charcoal, 12.6 pct in mass in the fraction smaller than 200 mesh. The amount of volatiles released from the wood charcoal was measured in conditions of fast heating following the same procedure described previously. Volatiles appear evenly distributed according to the sizes of the wood charcoal, ranging from 16.8 up to 18.6 pct. The composition of the ore used in given in Table II.

Table II. Composition of Ore Used in This Work

Analyte	Mass Percent
Total iron	70.13
MnO	0.08
SiO_2	3.38
Al_2O_3	0.12
CaO	0.13
MgO	0.13
P_2O_5	0.01

The pellets used in reduction experiments were prepared from master mixtures of carbon and iron oxide with carbon to oxide ratios close to 0.175 by mass. Experiments were done with furnace temperatures between 900 °C and 1280 °C, as typical of RHF operations, as reported by Grebe *et al.*[12] The wood charcoal and coal used were devolatilized at 1000 °C for 10 hours under a stream of argon prior to the preparation of the pellets. All reactants were sized to −200 mesh before mixing and agglomeration. The agglomeration of the pellets was done by addition of water followed by rolling and drying in a muffle furnace at 200 °C for 4 days. Pellets containing ore required addition of a binder (5 pct in mass of bentonite

containing sodium) for agglomeration. The final pellets used in reduction experiments had masses ranging from 2.0 to 5.0 g, providing for two ranges of diameters close to 1.0 and 1.6 cm.

During the pellet reduction experiments, changes in mass were recorded with the same procedure used previously. The composition of gas leaving the furnace tube was also monitored using a mass spectrometer linked to the gas outlet of the furnace. Changes in pellet size were measured by two different procedures. First, a caliper was used to measure the initial and final diameter of the pellets along four different directions. Changes in pellet size were also measured placing a charge-coupled device (CCD) camera in front of the observation window at the bottom of the reaction tube. The images from the camera were continuously registered in video cassete and later analyzed with an image analyzer where the cross-sectional area of the pellets was measured. The errors in all measurements were studied in detail and do not invalidate the conclusions drawn here.

Ancillary experiments were developed to study the heat-transfer conditions from the furnace to the surface of the pellets during fast heating after loading into the furnace. Conditions of heat transfer were studied placing an optical pyrometer in front of the observation window at the bottom of the reaction tube. These experiments were done with pellets of pure hematite so that chemical reactions did not affect the analysis of the data. In these experiments, the temperature readings from the pyrometer were continuously registered in a microcomputer linked to the pyrometer. Heat-transfer conditions were summarized in terms of the radiation heat-transfer coefficient pellet-furnace tube by best fit of the data acquired with a simple model for the heating of pellets in the absence of reactions resulting in a range of view factors from 0.6 to 1.0. The average value of 0.8 was used during the simulations of composite pellets.

III. MODEL DEVELOPMENT

In order to predict rates of reduction of composite pellets in an industrial RHF based on laboratory data and to cope with the variety of reduction patterns seen during the experimental work, a model of reduction was developed following the guidelines of previous researchers. As in previous works, two equations of continuity (for gas and solids) were coupled with the enthalpy balance in a control volume inside the composite assuming spherical symmetry for simplicity. The equations used for computation of changes in mass and temperature inside the composites were as follows:

$$\frac{\partial \rho_i}{\partial t} = -\frac{1}{h^2}\frac{\partial(\rho_i \nu_i h^2)}{\partial h} + r_i \quad [1]$$

$$\sum_{i=1}^{i=P}\frac{\partial \rho_i \overline{H}_i}{\partial t} = -\sum_{i=1}^{i=P}\frac{1}{h^2}\frac{\partial(\rho_i \nu_i h^2 \overline{H}_i)}{\partial h} + \frac{1}{h^2}\frac{\partial}{\partial h}\left(kh^2\frac{\partial T}{\partial h}\right) \quad [2]$$

where ρ_i represents the molar concentration of component i in the pellet (mol/m^3 of pellet), P represents the total number of components present in the pellet, t represents time (s), v_i is the velocity of species i along the radius of the pellet (m/s), h is the distance from the center of the pellet (m), r_i is the rate of formation of component i per unit volume of pellet (mol/m^3·s), $\overline{H}_i$ represents the molar enthalpy of compound i (J/mol), k represents the thermal conductivity of the pellet (J/s·m·K), and T represents the temperature (Kelvin) of the pellet at a given position h. In considering the possibility of shrinkage as suggested by Gilbert,[13] the identity in volume fractions of the several solids and void space inside the composite was considered:

$$g_P + \sum_{i=1}^{i=S} g_i = 1 \Rightarrow \sum_{i=1}^{i=S} g_i = 1 - g_P \quad [3]$$

where g_i represents the volume fraction of solid i in the mixture, S represents the total number of solid components in the mixture, and g_p represents the pore fraction of the mixture. Solid velocities could be computed by means of identity [3] and a known function for the total change in pore with time as

$$\frac{\partial g_P}{\partial t} = \sum_{i=1}^{i=S}\frac{1}{\psi_i}\left[\frac{\partial(\rho_i \nu_i)}{\partial h} + r_i\right] \Rightarrow$$

$$\sum_{i=1}^{i=S}\frac{1}{\psi_i}\frac{\partial(\rho_i \nu_S)}{\partial h} = \frac{\partial g_P}{\partial t} - \sum_{i=1}^{i=S}\frac{r_i}{\psi_i} \quad [4]$$

where ψ_i (mol/m^3) is the compact molar density of each solid in the mixture. Gas velocities were computed combining the equation of continuity for the gas phase with the ideal gas law:

$$\psi_i = \frac{P_i}{\mu T} \quad [5]$$

where P_i stands for the partial pressure of gas i in the mixture (Pa) and μ stands for the universal gas constant (Pa·m^3/mol·K). The resulting equation for gas velocity obtained is

$$\frac{\partial \psi_i g_P}{\partial t} = -\frac{\partial(\psi_i g_P \nu_i)}{\partial h} + r_i \quad [6]$$

In computing gas velocities, a total pressure of 101,325 Pa was assumed to hold during the entire process of reduction. This assumption was taken from the argument of Tien and Turkdogan[3] that significant pressure buildups should not occur inside reacting composites and the experimental measurements of Fruehan.[14] The equations obtained for changes in moles, temperature, and velocities of gas and solid were discretized according to the methodology of Patankar.[15] Briefly, the equations are first integrated over finite radial distances inside the pellet and suitable approximations for the derivatives of intensive properties at the boundaries are chosen for the computation of fluxes between control volumes. The derivatives in time were dealt with employing a fully explicit scheme.

In order to define the boundary condition of heat transfer to the surface of the pellets, the contributions due to convection and radiation outside the pellet were estimated from literature correlations. This analysis revealed that most heat transfer is due to radiation. Thus, the boundary condition used was defined as

$$q = S \cdot \varepsilon_F \cdot \varepsilon_P \cdot \sigma \cdot (T_F^4 - T_P^4) \quad [7]$$

where q is the heat flux (J/m^2·s·K) to the surface of the pellets, S is a geometric view factor ranging from 0 to 1, ε_F and ε_P are the emittances of furnace tube and pellet, σ is the Stefan–Boltzmann constant (J/m^2·s·K^4), and T_F and T_P are the temperatures of the furnace and pellet surface (K).

A literature search of emittances of carbon, oxidized iron, and alumina showed large ranges of values depending on specific conditions of the surfaces. Therefore, in analyzing heat transfer from the surroundings to the pellets, a heat-transfer coefficient (h_r) was defined as the product of emittances and view factor as

$$h_r = S \cdot \varepsilon_F \cdot \varepsilon_P \qquad [8]$$

The coefficient h_r in the experimental apparatus is in the range 0.6 to 1.0. This range was determined from the comparison of experimental results of surface temperature measurements of a pellet of pure hematite and results from the model developed. Thermal conductivities of the reacting composites were computed from the measurements in compact samples of iron oxides and iron done by Akyiama *et al.*[16] and a comparative literature study of values reported for carbon. It should be noticed that values reported for carbon span a considerable range from a low 0.84 for amorphous graphite to 418 J/m·s·K in recrystallized ingots. In this work, only the upper limit of 418 J/m·s·K was used in the simulations. The model chosen to represent the thermal conductivity of the aggregate assumed an arrangement of series resistances for the solid phases in parallel with pores of negligible conductivity based on Maxwell's electric analogy. Radiation through pores was disregarded from a comparison of results from Schotte's[17] correlation and the conductivity of the solid phases present. Finally, the contribution of interface resistances between grains suggested by Luikov *et al.*[18] was also disregarded from the results of experiments with samples of loose alumina and iron oxide powders in a unidirectional heat-transfer apparatus. The overall expression used for the thermal conductivity of the aggregate is

$$k = (1 - g_P) \frac{g_S}{\sum_S g_i/k_i} \qquad [9]$$

where g_S represents the sum of volume fractions of the solids in a given control volume, and k_i represents the thermal conductivity of each compact solid in the mixture. The values of k_i were taken from Akyiama *et al.*[18] the volume fractions of the several solids being computed from their compact densities (ψ_i) and concentrations inside the pellet (ρ_i). The interested reader is referred elsewhere to further details on the estimation of overall thermal conductivity of powder aggregates.[19]

IV. RESULTS AND DISCUSSION

A. *Reduction Rates*

Wood charcoal: Experimental measurements of mass loss and gas composition during reduction of pellets of wood charcoal and hematite or ore are shown in Figures 1 and 2. As can be seen in the figures, no sudden changes in slope indicating abrupt changes in reaction rates could be seen in the measurements of mass loss taken during experiments with these types of composite pellets. The absence of marked changes in reaction rates during the experiments strongly suggests that carbon oxidation is not the only rate-controlling mechanism in operation. In strict control by carbon oxidation,

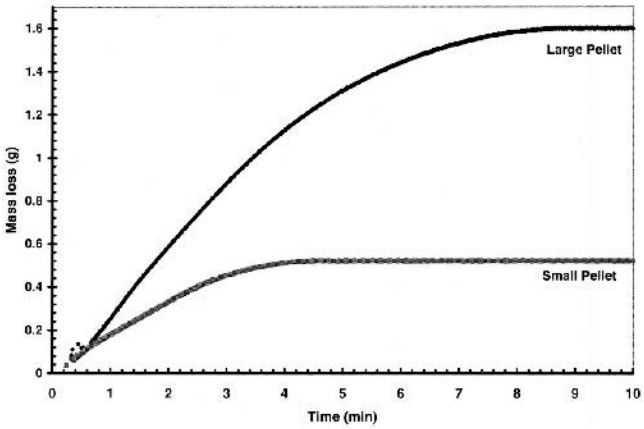

Fig. 1—Measurements of mass loss with a large (4.04 g) and a small (1.31 g) pellet of wood charcoal and hematite at 1200 °C.

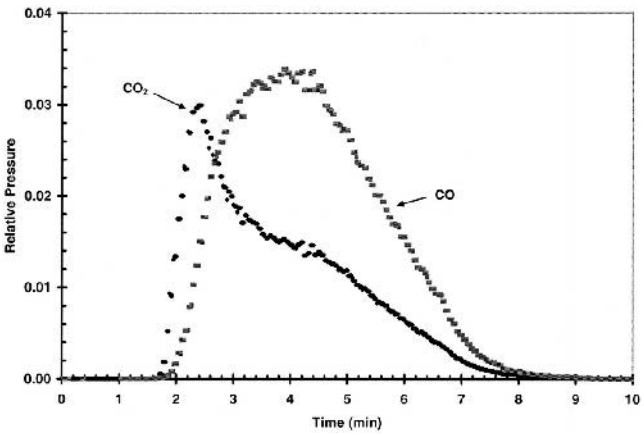

Fig. 2—Off-gas composition measurements from the experiment with a large pellet of wood charcoal and hematite (4.04 g at 1200 °C) in terms of the relative pressure ratio of CO_2 and CO to the pressure of argon in the purge gas (P/P_{Ar}).

at least one marked change in rate should be seen corresponding to the increase in CO content of the off-gas due to the transition between the steps of reduction of magnetite to wustite and wustite to iron. Indeed, rates of reaction per unit mass of carbon or iron oxides computed from the experimental data were not constant between experiments with large and small pellets at the same temperature, as should be expected from pure control by one of the two chemical steps. Instead, the best correlation found in pellets containing wood charcoal was between their initial surface area and the initial absolute rate (g/s). This empirical correlation is strong evidence that external heat transfer from the furnace tube to the samples plays a significant role in determining the overall rate of reaction. Measurements of off-gas composition showed an initial period with large generation of CO_2 followed by a short "plateau" and final decrease toward the end of reduction. These measurements of off-gas composition support the proposition of Rao[2] that reduction takes place following the stepwise transformation $Fe_2O_3 \rightarrow Fe_3O_4 \rightarrow$ "FeO" $\rightarrow$ Fe. A peculiarity was found in the cross sections of partially reduced pellets containing wood charcoal, as shown in Figure 3. As can be seen in Figure 3, a rim of iron close to the

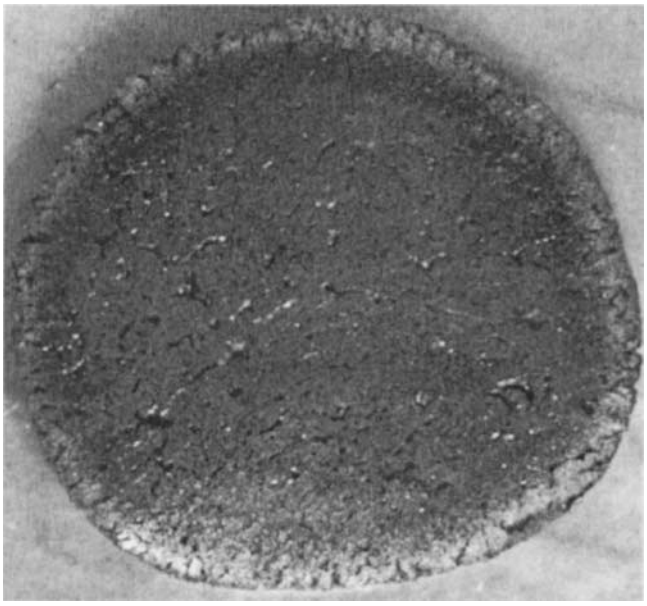

Fig. 3—Fracture surface of pellet containing wood charcoal and hematite showing a layer of reduced iron close to the surface.

surface of the pellet was found in pellets of wood charcoal resembling the outer topochemical layer found in pellets of pure iron oxides. The two observations of proportionality between the initial rates of reaction and presence of an outer rim of reduced iron may be considered experimental evidence of combined control by heat transfer to the surface and within the pellet.

Graphite: Typical results of measurements of mass loss and off-gas composition for pellets containing graphite are shown in Figures 4 and 5. In these experiments, the curves of mass loss indicate the existence of three main stages of reaction marked by two changes in slope. This observation is in support of the pattern proposed by Rao[2] with the changes in rate seen between the two first reaction stages (*i.e.*, the transformations of hematite to magnetite and magnetite to iron) explained by the change in CO concentration in the gas inside the composites; CO poisoning of carbon surfaces has been extensively reported as a cause for the retardation of rates of carbon oxidation. The increase in rate during the third reduction step indicated by the second change in slope cannot be explained by the effects of CO on the rates of carbon oxidation.

An ancillary set of experiments of graphite combustion in CO_2 was undertaken to clarify the possible existence of catalysis by iron formed during the third step of reduction as the motive for the increase in rate suggested by the second change in slope shown in Figure 4. The comparison of results from the experiments of graphite oxidation in CO_2 with the measurements of wustite reduction by graphite reported in Part I of this series of articles strongly suggested that catalysis by newly formed iron could play a part in this process. Rate constants of graphite oxidation measured after all corrections for mass-transfer effects were lower than measured in studies with composite samples with wustite in small crucibles. Therefore, catalysis of graphite by iron is a strong possibility to explain the rate increase observed. Another possibility for the rate increase observed during the

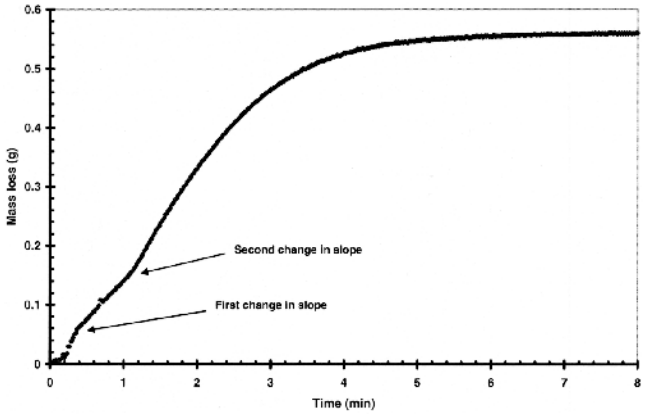

Fig. 4—Typical measurements of mass loss with pellets of graphite and hematite showing two changes in reaction rate (1.4 g pellet reduced at 1240 °C).

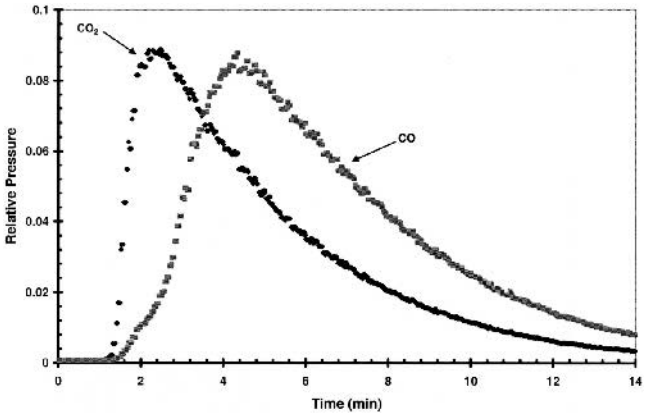

Fig. 5—Off-gas composition measurements from the experiment with a large pellet of graphite and hematite (3.98 g at 1240 °C) in terms of the relative pressure ratio of CO_2 and CO to the pressure of argon in the purge gas (P/P_{Ar}).

third reduction step is the development of extra porosity in the graphite. However, experiments with pellets at lower temperatures where heat transfer should play a lesser role in determining the overall reaction rate showed increases in rate of several orders of magnitude at sharply defined instants in time, as shown in Figure 6. An increase in graphite porosity of such magnitude occurring at the exact instant when the first formation of iron is expected seems unreasonable. Therefore, the catalytic activity of iron on the oxidation of graphite is the most plausible explanation for the increase in rate seen during the third stage of reduction of composite pellets.

Finally, differing from pellets with wood charcoal, no outer rim of iron could be identified in the cross sections of partially reduced pellets containing graphite, as exemplified in Figure 7. Rather, reduction seems to take place evenly throughout the specimen, suggesting the absence of significant gradients of gas composition and temperature.

Coal char: Results of mass loss and gas composition from experiments with pellets using coal char are shown in Figures 8 and 9. These results indicate that reaction rates of pellets containing coal char are roughly one order of

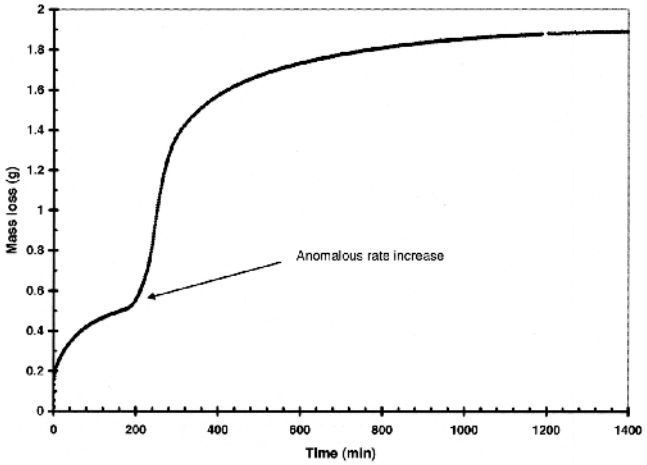

Fig. 6—Mass loss measured during reduction of hematite with graphite showing an anomalous rate increase (5.28 g at 900 °C).

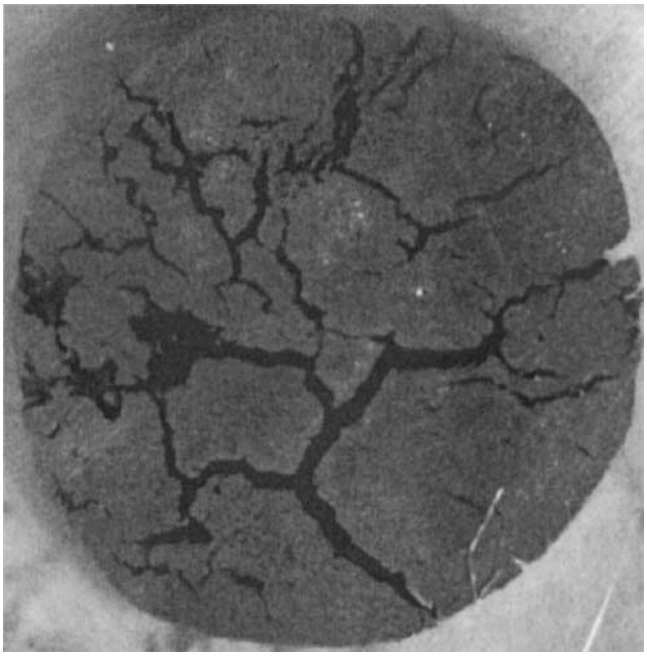

Fig. 7—Fractured surface of a pellet of graphite and hematite reduced up to approximately 50 pct of mass loss showing no appreciable differences in reduction extent.

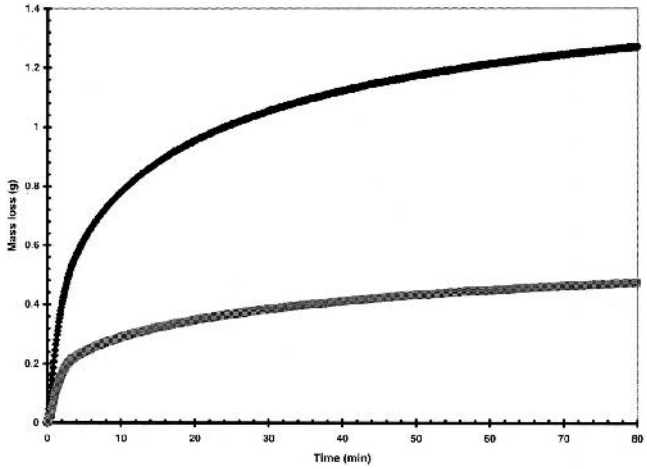

Fig. 8—Typical measurements of mass loss with pellets of coal char and hematite at a mass ratio coal char/hematite of 0.177 (pellets of 4.26 and 1.31 g reduced at 1200 °C).

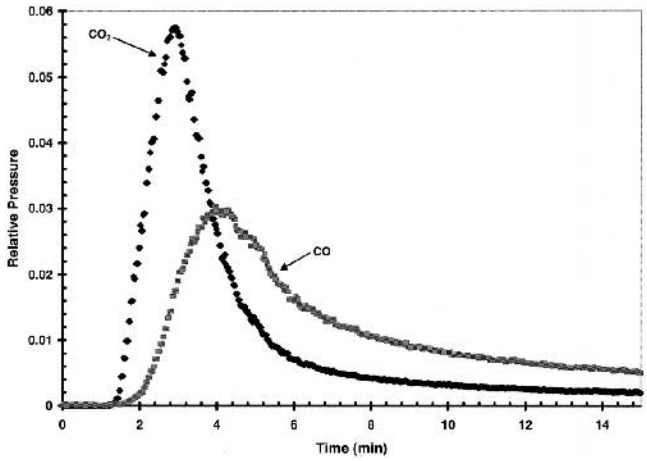

Fig. 9—Off-gas composition measurements from the experiment with large pellet of coal char and hematite (4.26 g at 1200 °C).

magnitude slower than rates in pellets containing wood charcoal. In general, these experiments showed one change in slope, indicating two main onsets of reaction. This is an indication of a reduction pattern following the sequence $Fe_2O_3 \rightarrow Fe_3O_4 \rightarrow Fe$ similar to that proposed by Fruehan[14] instead of the pattern $Fe_2O_3 \rightarrow Fe_3O_4 \rightarrow$ "FeO" $\rightarrow Fe$ followed in pellets with wood charcoal or graphite. This shift in reduction pattern is in agreement with the measurements of off-gas composition where an initial period with extensive formation of CO_2 is followed by a continuous decrease in the CO_2. In measurements with pellets containing coal char, no intermediate region with stable CO_2 amounts could be seen. Measurements of mass loss from pellets containing coal char did not show an increase in rate during the third stage of reaction, as should be expected from any catalytic effect of iron as during reduction by graphite. Finally, it was observed that reactions in pellets containing coal char are apparently much slower than in pellets with wood charcoal or graphite, as indicated by the much longer reaction times. This observation is in agreement with the observations of previous researchers that rates of coal char oxidation are slower than rates of oxidation of carbons from wood. Fractured surfaces of coal char pellets partially reduced were also examined and showed a uniform distribution of iron, suggesting the absence of significant gradients of temperature and gas composition.

B. *Pellet Shrinkage*

Owing to a considerable dispersion in the measurements of changes in diameter along the four different directions according to the placement of the pellets in the furnace tube, the extent of shrinkage among pellets of the same type was quantified in terms of a shrinkage coefficient (S_h) defined

as the ratio between the final (D_F) and initial (D_0) average diameters measured along the four directions as

$$S_h = \frac{D_F}{D_0} \qquad [10]$$

The values of shrinkage coefficients are given in Table III. As can be seen in the table, the experiments show the occurrence of some shrinkage in all types of pellets studied. The data summarized in Table III suggested that the type of iron oxide is important to the changes in size of the pellets, shrinkage being more pronounced in pellets containing hematite than in pellets containing ore. Indeed, a more careful analysis of shrinkage in terms of the change in cross section area of the pellets during reduction showed two distinct behaviors according to the type of iron oxide used.

Shrinkage was further studied by means of the measurements of cross section area from the images registered with the CCD camera. Examples of measurements in the cross-sectional area of pellets containing wood charcoal are shown in Figure 10 in terms of the relative change in area defined as the ratio between the instantaneous cross section measured and the initial cross section of the pellets. As exemplified in Figure 10, all experiments with pellets containing hematite showed an initial period of fast shrinkage regardless of the type of carbon used. This behavior was not seen in pellets containing ore, suggesting that the initial shrinkage is related to the sintering of the iron oxides. In some of the measurements of cross-sectional area with pellets containing ore, a small initial increase in cross-sectional area of less than 10 pct was observed, confirming the experimental observation of Seaton *et al.*;[20] this initial increase could be due to the thermal expansion of the iron oxides and carbon.

Table III. Computed Values of Average Shrinkage Coefficients for Different Types of Composite Pellets

Mixture	$S_h(\pm 0.04)$
Wood charcoal + ore	0.78
Wood charcoal + hematite	0.74
Coal char + ore	0.75
Coal char + hematite	0.73
Graphite + ore	0.83
Graphite + hematite	0.72

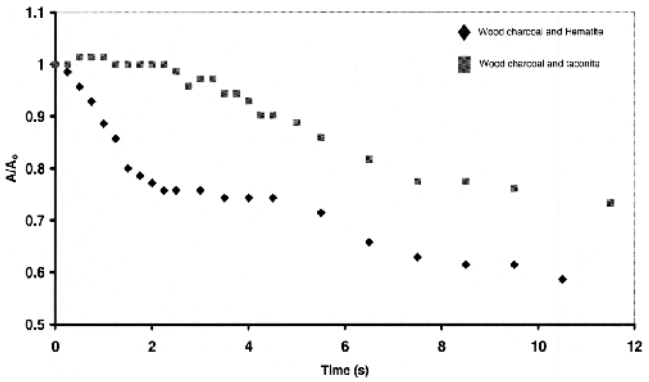

Fig. 10—Measurements of cross-sectional area of pellets of wood charcoal and hematite, and wood charcoal and North American ore showing distinct shrinkage patterns.

In order to set a maximum limit on the possible extent of shrinkage due to the sintering of the iron oxides, results from the experiments where a pellet of pure hematite was sintered for 20 hours in the reaction tube were used. Clearly, the long time allotted for the sintering of the hematite at the elevated temperature of the experiment would ensure the attainment of the upper limit of sintering shrinkage. For modeling purposes, an empirical correlation for the change in pore fraction of the hematite due to sintering was derived from the measurements of pellet diameter as

$$g_P = 0.8052 \times \exp(-6.80 \times 10^{-4}\, T) \qquad [11]$$

The preceding correlation was obtained assuming an exponential dependence for the volumetric fraction of pores on temperature, as introduced by Seaton *et al.*[20] The pore fractions of the initial and final hematite pellet were computed from the density of compact hematite and the measurements of pellet mass and diameter. Equation [11] was used in the reduction model of pellets containing hematite to account for the sintering of the iron oxides.

C. *Comparison to Model*

In order to evaluate the interplay among the several factors operating during the reduction of composite pellets, the model developed was first validated against experimental measurements of mass loss. Figures 11 and 12 show the comparison of results from the model with experimental results for pellets of hematite and wood charcoal or graphite at different reduction temperatures. Comparison between model results and experiments with different pellet sizes at different temperatures were equally satisfactory. The model developed was successful in simulating composites with hematite in all cases up to approximately 90 pct of reduction. In some cases, slower rates were measured after 90 pct reduction than were predicted from the model possibly due to the partial melting of the Fe-C alloys formed during reduction of the wustite. Also, as discussed in Part I of the current series of articles, these deviations could be due to the changes in porosity of the carbon and iron oxide particles

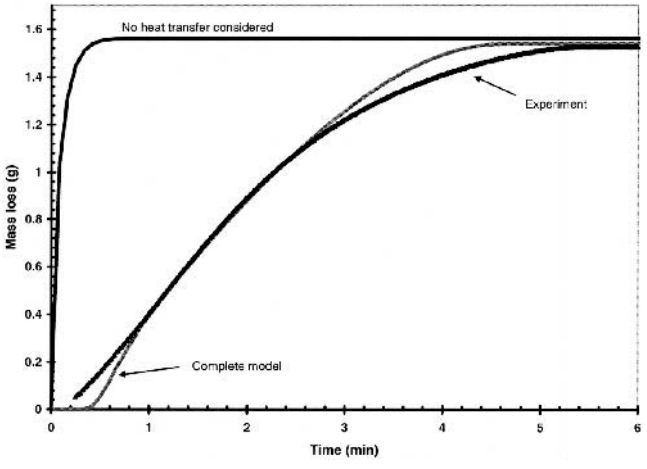

Fig. 11—Comparison of experiment and pellet model for a pellet of wood charcoal and hematite. Isothermal model included for illustrative purposes. Large pellet with 3.86 g reduced at 1280 °C. Wood charcoal/hematite mass ratio of 0.1766.

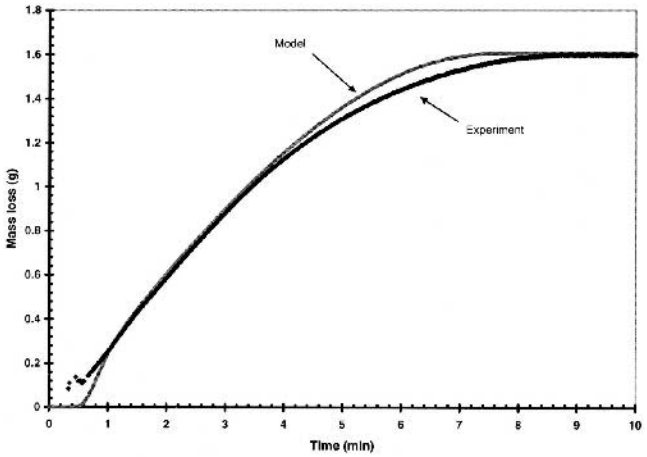

Fig. 12—Comparison of experiment and pellet model for a pellet of wood charcoal and hematite. Large pellet with 4.04 g reduced at 1200 °C. Wood charcoal/hematite mass ratio of 0.1766.

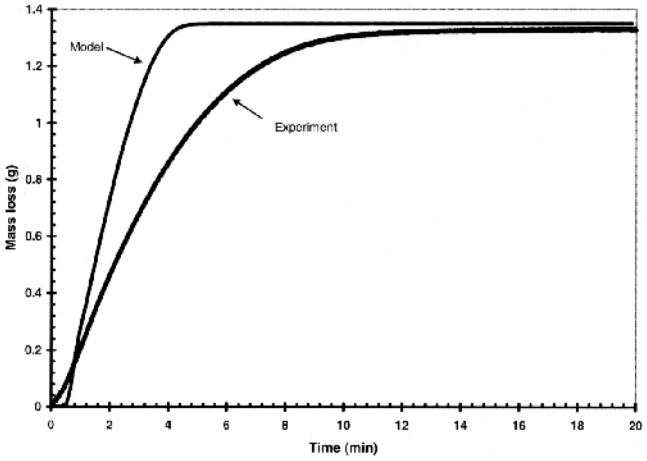

Fig. 13—Comparison of experiment and pellet model for a pellet of wood charcoal and ore. Large pellet with 3.97 g reduced at 1200 °C. Wood charcoal/ore mass ratio of 0.1769.

undergoing reactions. For illustrative purposes, Figure 11 also shows results from a calculation where heat-transfer effects are disregarded (*i.e.*, in this simulation, the pellet is assumed to reach the temperature of the furnace and there remain for the entire period of reaction). The results in Figures 11 and 12 show that heat-transfer plays an important role in determining reaction rates in pellets of hematite combined with wood charcoal or graphite.

The model predictions for pellets of ore in combination with wood charcoal or graphite resulted in significantly faster rates than actually measured, as exemplified in Figure 13. These findings are in complete opposition to the behavior expected in the presence of the binder necessary for agglomeration. Carvalho *et al.*[21] has associated the presence of sodium with the formation of highly reducible iron morphologies (whiskers), thus suggesting that intrinsic rates of reduction should increase in the presence of the bentonite used. Neither sodium nor bentonite have ever been reported to have any effect on the oxidation of carbon. Partial melting of the samples is the most probable cause of the discrepancies found. This reason should be considered as speculative in nature since a detailed thermodynamic study of the system is necessary in order to determine if low melting temperature phases would be stable in the presence of bentonite. This issue should be further studied along with the kinetics of formation of these new phases. The model developed presents good predictive results in cases where no such complex phases are present such as in the studies of pellets of hematite in combination with wood charcoal or graphite.

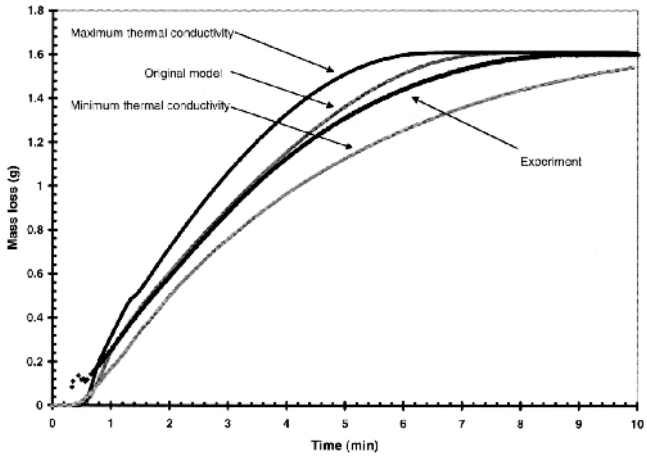

Fig. 14—Effect of changes in effective thermal conductivity on model predictions for a pellet of wood charcoal and hematite (4.04 g at 1200 °C).

The importance of heat transfer does seem dominant in experiments where good agreement with model predictions is found up to almost complete reduction. That is, while deviations should be expected for the reasons of extra area available for reactions and possible melting, the agreement is sustained up to almost complete reaction, indicating that other phenomena play a lesser role in determining overall reaction rates. In such cases, the agreement found suggests that intrinsic rates of reaction of carbon and iron oxides are fast enough to consume most of the heat supplied to the pellets.

In order to assess the relative importance of the two heat-transfer steps to the overall rate of reaction in composites of wood charcoal and hematite, calculations were done varying the heat-transfer coefficient (h_r) over the range 0.6 to 1.0 and the thermal conductivity of the pellet from 0.418 to 418 J/m·s·K. The importance of heat transfer inside the pellet to the overall reaction rate is exemplified by the results shown in Figure 14. The results shown in Figure 14 indicate that internal heat transfer has a significant role in the overall reduction rate attained. Indeed, among the factors studied, the internal condition of heat transfer was the one causing the most significant changes in model results. The evaluation of changes in the radiation heat-transfer coefficient representing the external condition of heat transfer showed that this parameter has little effect on the measured rates of reaction, as exemplified in Figure 15. Instead, the main effect of changes in view factor seems to be the change induced in the time necessary to attain significant rates of reaction. Effects of shrinkage were evaluated by comparison of results from simulations where it is disregarded with computations where it is taken into account, as well as with experimental measurements of mass loss. This comparison

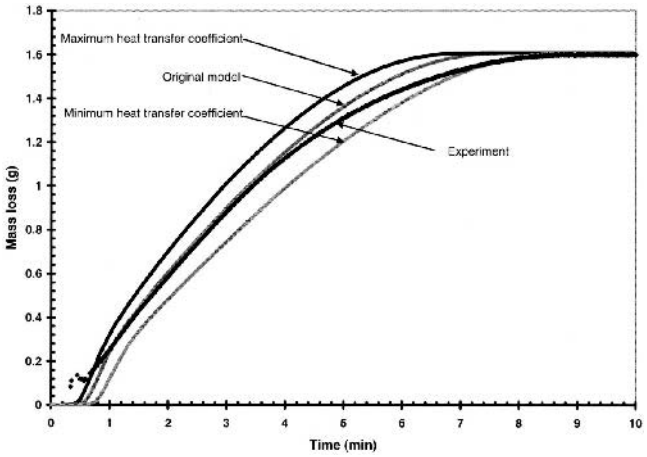

Fig. 15—Effect of changes in external heat-transfer coefficient on model predictions for a pellet of wood charcoal and hematite (4.04 g at 1200 °C).

showed that shrinkage introduces little change in the rates computed from the model. The deviations between the model and experimental results introduced by disregarding shrinkage are small and take place after 70 pct of mass loss.

V. SUMMARY AND CONCLUSIONS

In order to predict the rate of reduction of composite pellets of iron oxide and wood charcoal as proposed in the new process, a model of reduction for pellets was developed, including the most prominent features of models reported in the literature. The model developed includes chemical kinetics, heat transfer, and effects of pellet shrinkage. The intrinsic rate constants of carbon oxidation and reduction of wustite were measured in Part I of the current series of articles. Experimentally, studies of the reduction of composite pellets of wood charcoal, coal, and graphite in combination with hematite or ore were done to validate the model. The main conclusions from this work are as follows.

1. The assessment of compositions of off-gas during reduction confirmed the mechanism of gaseous intermediates as the main operative reaction mechanism in composite pellets.
2. The qualitative assessment of off-gas composition and mass change suggests that reduction in pellets of wood charcoal and graphite proceeds in the series $Fe_2O_3 \rightarrow Fe_3O_4 \rightarrow$ "FeO" $\rightarrow$ Fe, while in pellets with coal, it proceeds in the series $Fe_2O_3 \rightarrow Fe_3O_4 \rightarrow$ Fe.
3. The experimentally measured time to reach 90 pct reduction in pellets with coal char was 5 to 10 times longer than for pellets with wood charcoal, primarily due to the faster rate of oxidation of charcoal.
4. Rates of reduction in pellets with graphite are faster than rates of reduction in pellets with coal char, possibly due to the occurrence of catalysis of graphite oxidation by newly formed iron.
5. reduction model was developed taking into account the kinetics of carbon oxidation and reduction of wustite along with heat-transfer effects. This model was successfully applied to experiments done in the absence of binders.
6. Discrepancies found between results from the model and experimental measurements suggest that the presence of binder causes slower rates of reaction either by direct interaction with the reagents or by the formation of phases with low melting point.
7. For wood charcoal pellets reduced at temperatures common to RHF processes, the chemical rates of atomic recombination are fast, resulting in overall reaction rates controlled mainly by heat transfer. On the other hand, for pellets of coal char, the chemical rates are most probably the rate controlling step of the overall process.

ACKNOWLEDGMENTS

The authors thank the AISI-DOE, and the member companies of the Center for Iron and Steelmaking Research, for the sponsorship and collaboration. Also, the authors are very grateful to Professor Klaus Schwerdtfeger for all the help given in the development of the mathematical model. Finally, many thanks are due to Professor Alan Cramb for the help given in the experimentation concerning the determination of thermal conductivities.

REFERENCES

1. O.M. Fortini, and R.J. Fruehan: *Metall. Mater. Trans. B*, 2005, vol. 36B, pp. 865-72.
2. Y.K. Rao: *Chem. Eng. Sci*., 1974, vol. 29, pp. 1435-45.
3. R.H. Tien and E.T. Turkdogan: *Metall. Trans. B*, 1977, vol. 8B, pp. 305-13.
4. J. Gadsby, F.J. Long, P. Sleighton, and K.W. Sykes: *Proc. R. Soc. London*, 1948, vol. A193, pp. 357-76.
5. A.E. Reif: *J. Phys. Chem*., 1952, vol. 36, pp. 785-88.
6. H.Y. Sohn and J. Szekely: *Chem. Eng. Sci*., 1973, vol. 28, pp. 1789-801.
7. S. Sun and W.-K. Lu: *Iron Steel Int*., 1993, vol. 33 (10), pp. 1062-69.
8. S. Sun and W.-K. Lu: *Inst. Jpn. Int*., 1999, vol. 39 (2), pp. 130-38.
9. E. Donskoi and D.L.S. McKelwain: *Ironmaking and Steelmaking*, 2001, vol. 28 (5), pp. 384-89.
10. R.H. Spitzer, F.S. Manning, and W.O. Philbrook: *Trans. TMS-AIME*, 1966, vol. 236, pp. 1715-24.
11. Q. Wang, Z. Yang, J. Tian, W. Li, and J. Sun: *Ironmaking and Steelmaking*, 1998, vol. 25 (6), pp. 443-47.
12. K. Grebe, G. Gunter, H.-J. Lehmkuhler, and H. Schmauch: *Stahl Elsen*, 1990, vol. 110 (7), pp. 99-106.
13. D. Gilbert: *Iron Ore for Alternative Iron Units*, Gorham Intertech Conf., Charlotte, NC, Oct. 25–27, 1999.
14. R.J. Fruehan: *Metall. Trans. B*, 1977, vol. 8B, pp. 279-86.
15. S.V. Patankar: *Numerical heat transfer and fluid flow*, Taylor & Francis, New York, NY, 1980.
16. I. Akyiama, H. Ohta, R. Takahashi, Y. Waseda, and J.-I. Yagi: *Iron Steel Inst. Jpn. Int*., vol. 32(1992), No. 7, pp. 829-37.
17. W. Schotte: *A IChE J*., 1960, vol. 6, pp. 63-66.
18. A.V. Luikov, A.G. Shashkov, L.L. Vasiliev, and Y.E. Fraiman: *Int. J. Heat Mass Transfer*, 1968, vol. 11, pp. 117-40.
19. O.M. Fortini: "Renewable Energy Steelmaking: on a New Process for Ironmaking," Carnegie Mellon University, Pittsburgh, PA, 2004.
20. C.E. Seaton, J.S. Foster, and J. Velasco: *Trans. Iron Steel Inst. Jpn*., 1983, vol. 23, pp. 490-96.
21. R.J. Carvalho, P.G. Quariguasi Netto, and J.C. d'Abreu: *Can. Metall. Q*., 1994, vol. 33 (3), pp. 217-25.
22. O.M. Fortini and R.J. Fruehan: *Steel Res. Int*., 2004, vol. 75 (10), pp. 625-31.